

Fundamental Differences in Dedifferentiation and Stem Cell Recruitment during Skeletal Muscle Regeneration in Two Salamander Species

Tatiana Sandoval-Guzmán,^{1,4} Heng Wang,^{3,4} Shahryar Khattak,^{1,2,4} Maritta Schuez,^{1,2} Kathleen Roensch,¹ Eugeniu Nacu,¹ Akira Tazaki,¹ Alberto Joven,³ Elly M. Tanaka,^{1,*} and Andrés Simon^{3,*}

¹Technische Universität Dresden, DFG Research Center for Regenerative Therapies, CRTD

²Max Planck Institute of Molecular Cell Biology and Genetics, 01307 Dresden, Germany

³Department of Cell and Molecular Biology, Centre of Developmental Biology for Regenerative Medicine, Karolinska Institute, SE-171 77 Stockholm, Sweden

⁴These authors contributed equally to this work

*Correspondence: elly.tanaka@crt-dresden.de (E.M.T.), andras.simon@ki.se (A.S.)

<http://dx.doi.org/10.1016/j.stem.2013.11.007>

SUMMARY

Salamanders regenerate appendages via a progenitor pool called the blastema. The cellular mechanisms underlying regeneration of muscle have been much debated but have remained unclear. Here we applied *Cre-loxP* genetic fate mapping to skeletal muscle during limb regeneration in two salamander species, *Notophthalmus viridescens* (newt) and *Ambystoma mexicanum* (axolotl). Remarkably, we found that myofiber dedifferentiation is an integral part of limb regeneration in the newt, but not in axolotl. In the newt, myofiber fragmentation results in proliferating, PAX7⁻ mononuclear cells in the blastema that give rise to the skeletal muscle in the new limb. In contrast, myofibers in axolotl do not generate proliferating cells, and do not contribute to newly regenerated muscle; instead, resident PAX7⁺ cells provide the regeneration activity. Our results therefore show significant diversity in limb muscle regeneration mechanisms among salamanders and suggest that multiple strategies may be feasible for inducing regeneration in other species, including mammals.

INTRODUCTION

In salamanders, limb amputation causes the formation of a proliferative progenitor cell zone called the blastema that faithfully regenerates the original limb (Stocum and Cameron, 2011). Whether blastema cells arise from resident adult stem cells or by cellular dedifferentiation has long been debated and skeletal muscle has been an intense focus of such studies (Slack, 2006). Conclusive, quantitative evidence for skeletal muscle dedifferentiation was lacking, due to the inability to long-term fate map endogenous muscle fibers. Histological and short-term cell labeling studies suggested that multinucleated myofibers and implanted myotubes dedifferentiate into mononuclear, proliferative cells in the first weeks of limb and tail regeneration (Calve

and Simon, 2011; Echeverri et al., 2001; Hay, 1959; Lo et al., 1993). The results of implantation of virally marked myotubes were also consistent with fragmentation and proliferation (Kumar et al., 2000). In vitro, newt myotube nuclei could be stimulated to reenter the cell cycle (Tanaka et al., 1997) and several conditions could induce myotube fragmentation into smaller myotubes or mononuclear cells (Calve et al., 2010; Duckmanton et al., 2005; Kumar et al., 2004; Odelberg et al., 2000). On the other hand, PAX7⁺ satellite cells exist in salamander muscle tissue and become proliferative upon amputation (Morrison et al., 2006). Implantation of cultured satellite cells contributed to regeneration but the fate of endogenous PAX7⁺ cells was not clear (Kragl et al., 2009; Morrison et al., 2006, 2010).

Here we describe *Cre-loxP*-based genetic fate mapping of muscle during limb regeneration in two salamander species, *Notophthalmus viridescens* and *Ambystoma mexicanum*. Surprisingly, in the newt, *Notophthalmus viridescens*, muscle dedifferentiation makes a significant contribution to muscle regeneration, while in the axolotl, *Ambystoma mexicanum*, myofibers make no contribution to limb regeneration and PAX7⁺ satellite cells are the main contributor to axolotl limb muscle regeneration. These results reveal an unexpected evolutionary diversity in muscle dedifferentiation among closely related species.

RESULTS

Myofibers Contribute to Regenerated Muscle in the Newt Limb

Our aim was to permanently mark muscle fibers in the newt limb and follow them through regeneration. To genomically integrate a Cherry-to-nlsYFP *loxP* reporter, we flanked the *loxP* expression cassette with *ToI2* transposon sites and coelectroporated limb tissue with a *ToI2* transposase expression vector (Figure 1A) (Kawakami, 2007). In addition, the electroporation mix contained a *Cre* expression plasmid: either a muscle-specific *Cre* expression vector, *MCK:Cre* (Jaynes et al., 1988); a ubiquitously expressed *CMV:Cre* plasmid; or control empty *PUC19* vector (Figure 1A). Importantly, the transposase and the *Cre*-driver vectors did not contain transposase sites, and therefore would be transiently expressed. Therefore,

only the *loxP* expression cassette would integrate long-term into the genome of the limb cells.

We first confirmed that YFP expression from the *loxP* reporter depended on CRE activity and that expression lasted through regeneration. When the *loxP* reporter was coexpressed with empty *PUC19* in the mature limb, no YFP⁺ cells were observed (Figures 1A and 1B). In contrast, when the ubiquitously expressed *CMV:Cre* was used, nuclei both within and outside of muscle were labeled (Figures 1A and 1C). Upon amputation of *CMV:Cre* limbs, we detected nuclear YFP signal in multiple cell types of the 2-month-old regenerates, including skeletal muscle (Figures S1B and S1C, available online), epidermis (Figures S1D and S1E), and cartilage (Figures S1E and S1F). These results showed that we could trace the progeny of stump cells into the regenerate long-term.

We next assessed the specificity of the muscle *Cre*-driver, *MCK:Cre*, which yielded nuclear YFP⁺ expression exclusively in skeletal muscle as determined by coimmunostaining with Myosin Heavy Chain (MHC) (Figure 1D). YFP⁺ nuclei in muscle were only detected within the laminin⁺ basement membrane (Figure 1E) and they colocalized with the myogenic transcription factor MEF2C (Figure 1F). Of 642 YFP⁺ nuclei ($n = 5$ limbs), all were found within the basement membrane, and 561 out of 563 YFP⁺ nuclei were MEF2C⁺.

It was also important to confirm that PAX7⁺ satellite cells were not targeted by our labeling method. The electroporation conditions we employed were in fact unable to access satellite cells, as PAX7⁺ cells never expressed Cherry from the *loxP* reporter when the *loxP* reporter was electroporated alone (Figure S2A, $n = 208$ PAX7⁺ nuclei). We also did not find any YFP⁺PAX7⁺ cells after coelectroporation of the *loxP* reporter with *CMV:Cre* (data not shown). Consistent with these observations, electroporation of the *loxP* reporter and *MCK:Cre* yielded no YFP⁺PAX7⁺ nuclei (833 YFP⁺ nuclei in five limbs) (Figure S2B). We further confirmed these results in an in vitro culture of dissociated limb myofibers (Figures S2C and S2D). In such preparations, we counted 249 YFP⁺ nuclei out of 4,399 DAPI nuclei associated with myofibers and none were PAX7⁺ (Figure S2E). These in vitro studies also indicated that an average of $5.0\% \pm 1.6\%$ of dissociated myofibers expressed YFP ($n = 4$ limbs). These data collectively show that we could specifically target myonuclei in newt limb skeletal muscle.

Having shown the specificity and durability of the labeling method, we used it to trace myofibers during limb regeneration by coelectroporating upper arms with *MCK:Cre*, the *loxP* reporter, and the transposase constructs 14 days before amputation. To map the long-term fate of the myofiber-derived progeny, we analyzed limbs at the late palette and the late digit stages of regeneration (Iten and Bryant, 1973). Figure S3A shows the developing humerus, ulna, and radius, outlined by collagen-II staining in late palette stage regenerate where myogenesis was not yet complete. We detected YFP⁺ nuclei both proximally and distally to the level of amputation. Double immunostaining against collagen-II showed that YFP⁺ nuclei never colocalized with regenerating cartilage (Figure S3B), which was in contrast to the observations after *CMV:Cre*-mediated recombination (Figure S1F). When late digit stage regenerates were analyzed, we detected YFP⁺ nuclei in myofibers along the entire

proximal-distal axis, except at the digit tips (Figures 1G–1L). On average $5.33\% \pm 1.37\%$ of the myofibers were labeled throughout the limb excluding the fingertips (Figure 1M) and YFP⁺ nuclei were only found in myofibers. It is likely that the lack of YFP⁺ nuclei in the fingertips is due to the fact that there is almost no muscle found in this region. These data showed that myofibers quantitatively contributed to new muscle formation during newt limb regeneration.

Myofibers Dedifferentiate into Proliferative Blastema Cells during Newt Limb Regeneration

An important question is whether the injured myofibers dedifferentiate during the regeneration process. To test this, we first asked if YFP⁺ cells in the 2-week-old blastema had lost the muscle marker MHC (Figure 2A). Proximal to the amputation plane, we found YFP⁺ nuclei both within and around MHC⁺ myofibers (Figures 2B and 2E). At the base of the blastema, close to the amputation plane, we detected evidence of skeletal muscle fragments that were positive for MHC and contained YFP⁺ nuclei (Figures 2B and 2D). Importantly, in the distal blastema we observed YFP⁺ cells that were negative for MHC expression, indicating that muscle cells dedifferentiate to form mononuclear, blastema cells (Figures 2B and 2C).

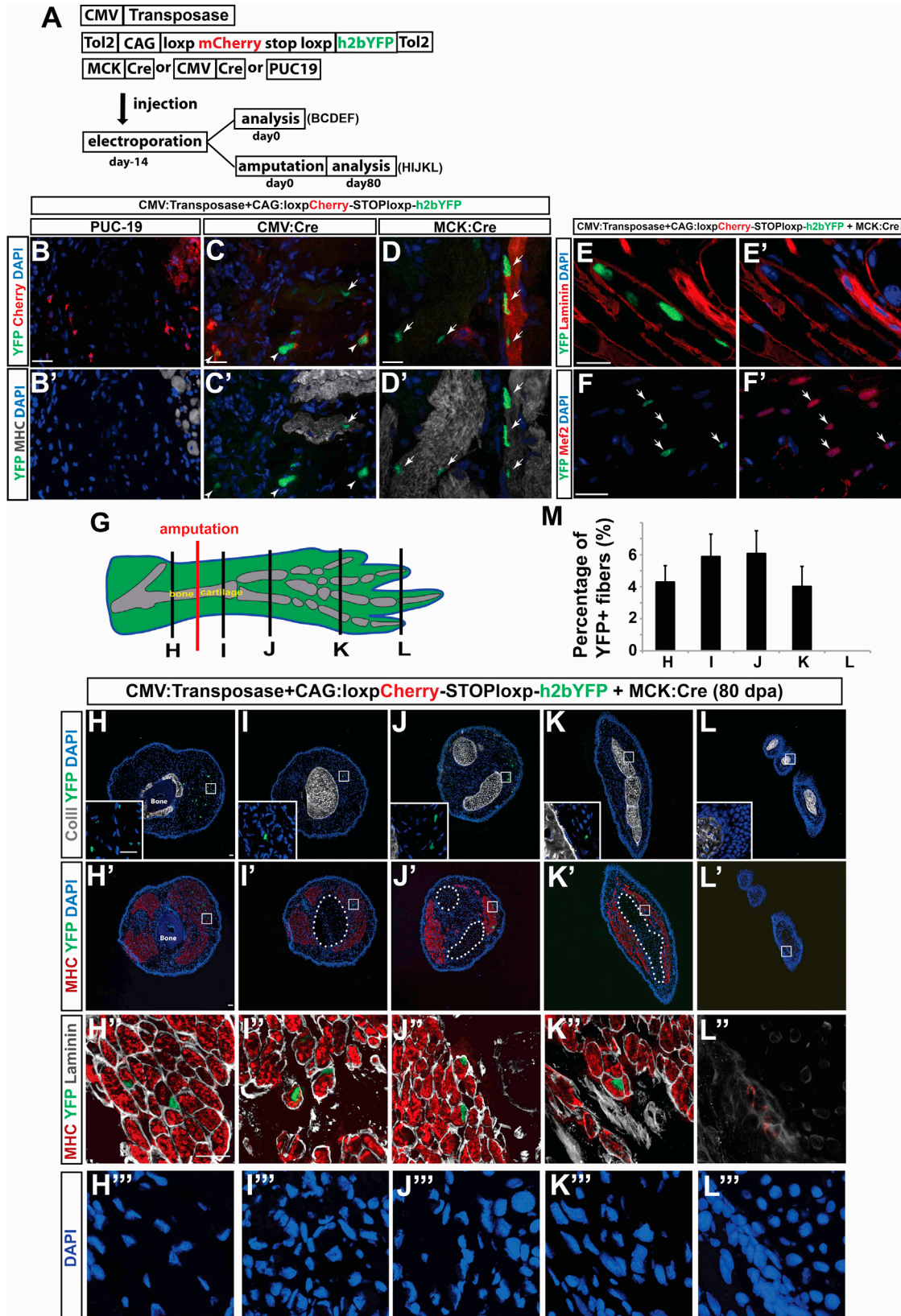
To determine if the YFP⁺MHC⁻ blastema cells were proliferative, we double immunostained for YFP and the proliferating cell nuclear antigen (PCNA). $16.7\% \pm 2.3\%$ ($n = 4$ limbs) of the YFP⁺ nuclei in the blastema were double positive, indicating that they were cycling (Figures 2F and 2G). We corroborated this conclusion by pulsing the animals with the nucleotide analog EdU using two different time windows. A short, 6 hr pulse on the day of sacrifice resulted in $8.0\% \pm 4.0\%$ ($n = 4$ limbs) of YFP⁺MHC⁻ cells incorporating EdU. Daily administration of EdU from 7 to 14 days postamputation (dpa) increased the fraction of EdU⁺YFP⁺MHC⁻ cells to $65.0\% \pm 13.3\%$ ($n = 3$ limbs) (Figures 2H and 2I). In the stump region, we never detected YFP⁺EdU⁺MHC⁺ nuclei, neither in MHC⁺ skeletal muscle fragments nor in intact myofibers, indicating that cell cycle reentry is a postfragmentation event localized to the blastema.

To determine the long-term fate of the YFP⁺EdU⁺ cells, limbs that had been pulsed with EdU during blastema formation (day 8–21) were analyzed at the late digit stage (80 dpa) (Figure 2A). We observed EdU⁺YFP⁺ nuclei within regenerated muscle in all regions of the new limb, including the hand, in two out of four samples (Figures 2J and 2K). In seven transverse hand sections we saw that 8 out of 27 labeled myofibers contained EdU⁺YFP⁺ myonuclei, indicating that the proliferating YFP⁺ cells had contributed to de novo myogenesis.

These data show that upon limb amputation, myofiber dedifferentiation produces MHC⁻, proliferative blastema cells that contribute to de novo muscle regeneration during limb regeneration in newts. The further molecular profile of the dedifferentiated, myogenic blastema cell is described later in this work.

Muscle Dedifferentiation Does Not Contribute to Limb Regeneration in Axolotl

The axolotl (*Ambystoma mexicanum*), another salamander species commonly used to study limb regeneration, presented additional opportunities to study muscle dedifferentiation. To initially assess whether axolotl myofibers contribute to limb regeneration



(legend on next page)

similarly to the newt, we performed electroporation-based muscle labeling. The *MCK:Cre*, *CAGGS:loxPCHERRY-STOPloxP-H2BYFP* and *CMV:Tol2-transposase* expression plasmids were coelectroporated into the axolotl limb (Figure 3A). Electroporated limbs showed robust nuclear YFP expression closely associated with myofibers as visualized by immunocytochemistry against MEF2C (Figures 3B–3D) or muscle-specific MHC (Figure 3E). Labeled limbs were amputated in the upper arm, allowed to regenerate fully, and then visualized both by whole-mount imaging at 33 dpa ($n = 5$, Figure 3F) and by sectioning of entire regenerated limbs at 90 dpa. In contrast to the results from the newt, nuclear counts along the sectioned regenerate showed that all visible YFP⁺ nuclei (732) were restricted to the upper limb region and no labeled nuclei were found in the distal upper arm, lower arm, or hand (Figures 3F and 3G). These results surprisingly suggested that myofibers make no contribution to the axolotl limb regenerate.

Considering the striking lack of myofiber contribution in axolotl, we sought to confirm our tracing results using germline transgenic animals (Sobkow et al., 2006). We have recently generated germline transgenic *loxP*-reporter animals, *CAGGS:loxP-GFP-STOP-loxP-Cherry*, and tamoxifen-inducible *Cre* lines including *CAGGS:ert2-cre-ert-T2A-nucGFP* (Khattak et al., 2013). Using these well-characterized animals, we achieved muscle-specific labeling by exploiting the syncytial property of differentiated skeletal muscle cells that form by myoblast fusion (Figure S4A and described further below). Conceptually, if we allow fusion of a *CAGGS:loxP-GFP-STOP-loxP-Cherry* myoblast with a *CAGGS:ert2-cre-ert-T2A-nucGFP* myoblast, the nuclei of the two genotypes would share a common cytoplasm, allowing the inducible CRE protein from one nucleus to enter the *CAGGS:loxP-GFP-STOP-loxP-Cherry* transgenic nucleus. Upon tamoxifen induction recombination would occur, resulting in Cherry expression throughout the myofiber cytoplasm.

We achieved cell-fusion-mediated muscle-specific labeling of *CAGGS:loxP-GFP-STOP-loxP-Cherry* and *CAGGS:ert2-cre-ert2-T2A-nucGFP* myoblasts by grafting an upper arm blastema from one genotype onto the upper arm stump of a host animal of the other genotype (“Axolotl LB-transplant,” Figure 4A). The grafted limbs were then allowed to fully regenerate. After grafting and limb differentiation, we did not observe Cherry⁺ cells in the limb prior to tamoxifen injection (Figures S4B and S4C). When

tamoxifen was injected into the animals, we observed strong Cherry expression in linear elements within the limb consistent with labeling of myofibers (Figures 4B and 4C). Both donor: host pairings, *CAGGS:loxPGFP-STOPloxPCherry::CAGGS:ert2-cre-ert2-T2A-nucGFP* or vice versa, gave muscle labeling ($n = 20$, $n = 13$ respectively). We did not observe any Cherry⁺ cells when the donor or host was replaced by a nontransgenic animal and induced with tamoxifen (Figures S4D–S4F).

The specificity of Cherry expression in muscle was confirmed by colocalization of the Cherry signal with muscle markers. Excellent colocalization of Cherry signal with MHC was observed, and no Cherry signal was observed outside of muscle tissue (Figures S5A–S5D). We also examined cross-sections for colocalization of Cherry signal with immunofluorescence signal for the nuclear muscle marker MEF2C or the satellite cell marker PAX7. For a total of 513 Cherry⁺ nuclei counted, 509 were found to be MEF2C⁺ (Figures S5E–S5H, $n = 11$ limbs). Conversely, for a total of 861 Cherry⁺ nuclei counted, two were found to be potentially PAX7⁺ (Figures S5I–S5L, $n = 9$ limbs). These results indicate that the cell labeling based on fusion of blastema cells with host cells during limb redifferentiation is muscle specific.

We then assessed the percentage of nuclei in the Cherry⁺ myofibers that had the genotype *CAGGS:loxP-Cherry*. In mature myofibers, transcripts and proteins show enrichment close to the nucleus producing a given transcript (Rossi et al., 2000). We therefore counted Cherry⁺ myofiber nuclei that showed very strong versus weaker signal. Out of 879 counted nuclei (six animals), 43% ± 10% of nuclei showed very strong nuclear Cherry signal (Figures S5M–S5P). This data indicates that we had an efficient conversion of the *loxP* cassette and a good yield in Cherry-expressing nuclei in limb myofibers.

To determine the contribution of myofibers to the limb regenerate, we amputated the labeled limbs in the upper arm and allowed regeneration to occur. Limbs were visualized by whole-mount microscopy and cross-section. Whole-mount visualization by widefield microscopy indicated that the visible Cherry⁺ myofibers were restricted to the upper arm of the regenerate and no signal was observed in the lower arm and hand (Figures 4D and 4E; Figures S6A–S6C, $n = 4$). Fluorescence intensity measurements along the proximal-to-distal limb axis showed high levels of Cherry⁺ fluorescence in the upper limb segment up to the amputation plane, while in the lower arm and hand, fluorescence levels dropped to those matching the contralateral

Figure 1. Long-Term Contribution by Myofibers to Limb Regeneration in Newts

- (A) Schematic outline of the experimental paradigms. Letters within parenthesis indicate the panels depicting the outcomes of the alternative procedures.
- (B) Only Cherry⁺ cells are visible when no *Cre* recombinase is expressed.
- (C) Cells within and outside of skeletal muscle are YFP⁺ when *Cre* recombinase is under the control of the ubiquitous CMV promoter. Arrowheads point to YFP⁺ nuclei outside of skeletal muscle in (C) and arrows point to YFP⁺ nuclei within skeletal muscle in (C) and (D).
- (D) Only cells in skeletal muscle are YFP⁺ when *Cre* is under the control of the muscle-specific MCK promoter. Dual Cherry and YFP expression indicates that not all copies of the *loxP* construct have converted to YFP.
- (E) YFP⁺ nuclei are located within the laminin⁺ basement membrane.
- (F) YFP⁺ nuclei are MEF2C⁺. Arrows point to colocalization.
- (G) Drawing of the location of the transverse sections shown in (H)–(L).
- (H) YFP⁺ nuclei in stump muscle.
- (I–K) YFP⁺ nuclei at the indicated levels (in G) along the proximo-distal axis.
- (L) Lack of YFP⁺ nuclei in the fingertip region.
- Dotted lines in (I')–(K') indicate the cartilage boundary. The inserts in (H')–(L') are shown in (H'')–(L'') and (H''')–(L''').
- (M) Graph showing the fraction of labeled myofibers at the indicated levels (in G) along the proximo-distal axis. Data are presented as mean ± SEM ($n = 4$). Scale bars: 20 μm. See also Figures S1, S2, and S3.

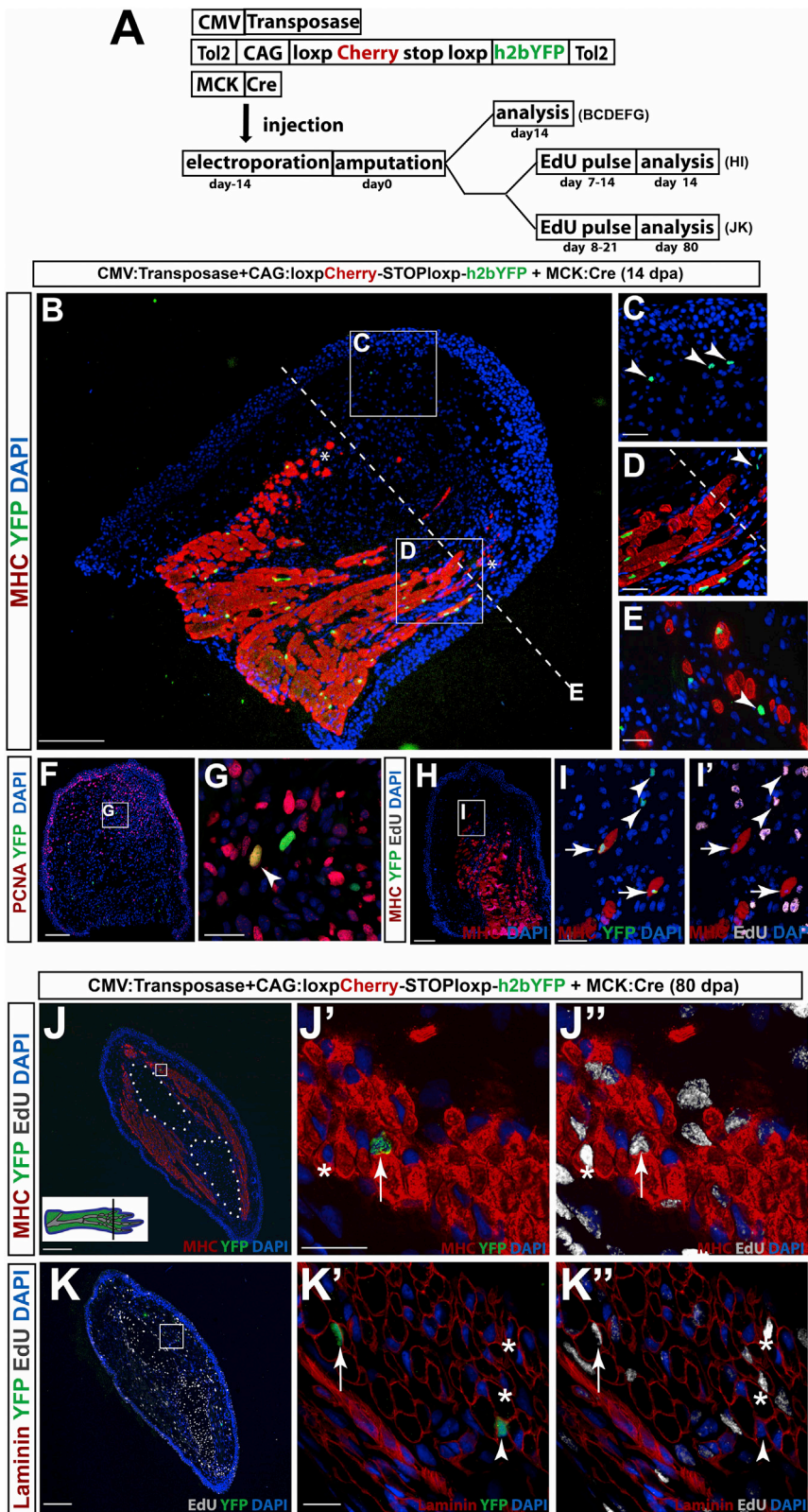


Figure 2. Myofibers Contribute Proliferating Cells to the Regenerating Newt Limb

(A) Schematic outline of the experimental paradigms. Letters within parenthesis indicate the panels depicting the outcomes of the alternative procedures.

(B) Overview in longitudinal section of a 14-day regenerate shows typical figures of fragmenting skeletal muscle during blastema formation. Dashed line indicates the amputation plane. Asterisks indicate fragmenting myofibers.

(C) Close-up of region C in the overview (B) shows examples of YFP^+MHC^- mononuclear cells in the distal blastema.

(D) Close-up of region D in the overview (B) shows YFP^+ nuclei within and outside of MHC^+ fragments.

(E) YFP^+MHC^+ and YFP^+MHC^- nuclei in a representative cross-section around the stump/blastema boundary. Arrowheads in (C)–(E) point to YFP^+MHC^- cells.

(F and G) Example of a $PCNA^+YFP^+$ cell (arrowhead) in the blastema.

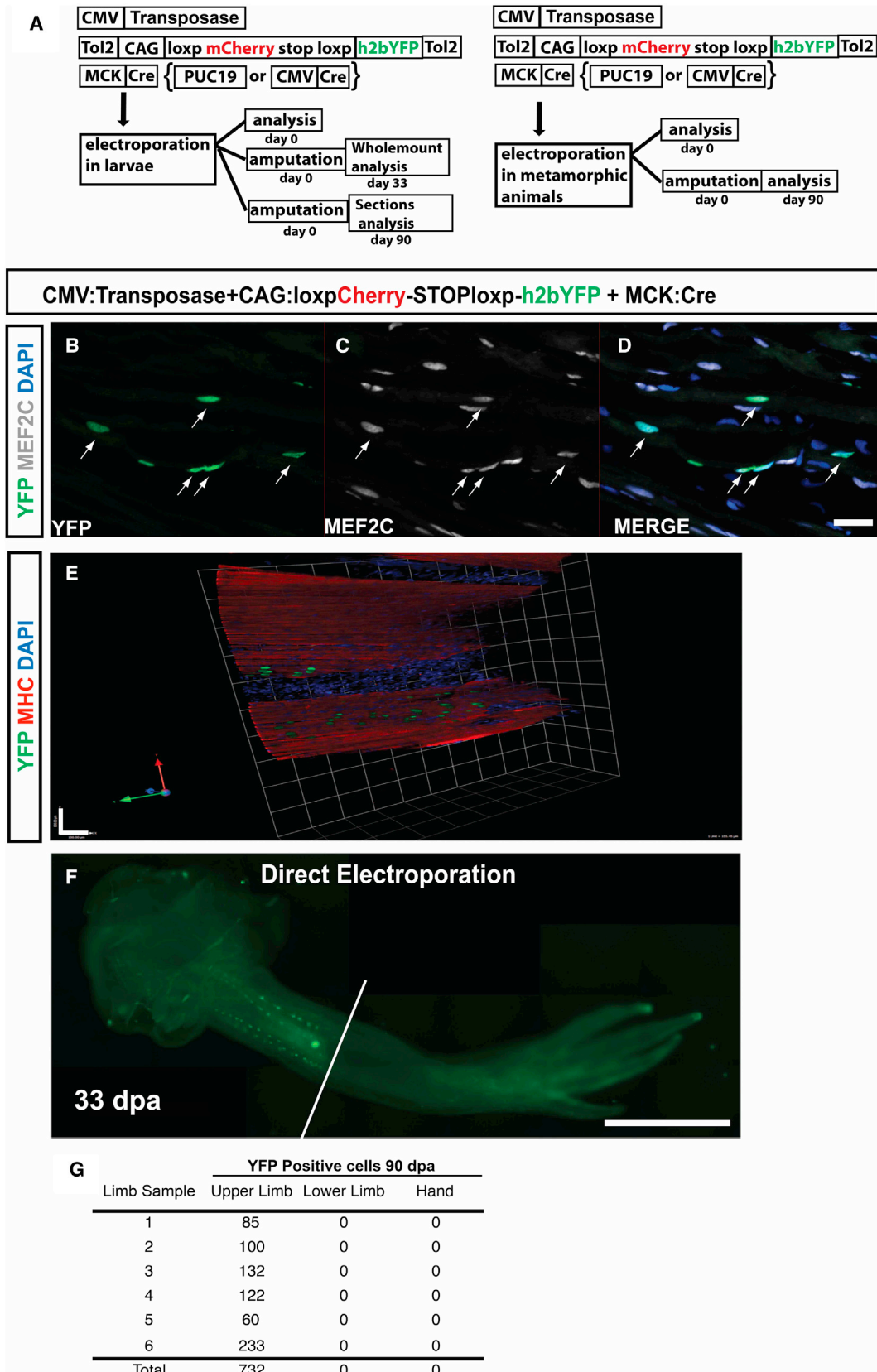
(H and I) EdU^+YFP^+ (arrowheads) mononuclear cells in the blastema and EdU^-YFP^+ (arrows) nuclei within the muscle.

(J) Examples of YFP^+EdU^+ and YFP^-EdU^+ myonuclei in MHC^+ myofiber in the hand region (region K in Figure 1).

(K) Examples of a YFP^+EdU^+ , YFP^+EdU^- , and YFP^-EdU^+ nuclei within the laminin $^+$ basal membrane in a myofiber in the hand region.

In (J) and (K), arrows point to YFP^+EdU^+ , arrowheads point to YFP^+EdU^- , and asterisks point to YFP^-EdU^+ myonuclei.

Scale bars, (B), (F), (H), (J), and (K): 200 μ m; (C–E), (G), (I), (J'), and (K'): 20 μ m.



(legend on next page)

control limb that had not received a blastema transplant (Figure 4F; Figure S6D). We also cross-sectioned regenerated limbs and quantitated the percentage of MHC⁺ myofibers that were Cherry⁺ at different levels along the amputated limb (Figures 4G–4K, n = 3). At the amputation plane, an average of 21% ± 15% of MHC⁺ myofibers strongly expressed Cherry. In contrast, we observed no MHC⁺Cherry⁺ myofibers in the lower arm and hand in the regenerates. These tracing results using germline transgenic animals confirm that myofibers make no detectable contribution to the regenerated axolotl limb.

Though we had not observed any labeled muscle in the regenerated limb, we examined the limb blastema for any possible evidence of muscle-derived mononucleate, proliferative cells as was found in the newt. We examined longitudinal sections of 10-day blastemas derived from LB-transplant animals. In contrast to the newt data, we found no labeled cells in the distal portion of the axolotl limb blastema (Figure S7A, n = 9). Among nine samples examined, all Cherry⁺ fragments that potentially represented mononucleate cells were located close to the amputation plane and none were found in the mid or distal blastema. Only 164 out of 580 Cherry⁺ fragments colocalized with a Hoechst⁺ nucleus (Figures S7A–S7C). Furthermore, none of the Cherry⁺ signal was associated with a PCNA⁺ nucleus (Figures S7A–S7C) and no Cherry⁺ signal was found colocalizing with PAX7⁺ blastema cells (Figures S7D–S7F). In summary, our results indicate that axolotl myofibers undergo considerable morphological changes at the amputation plane, but we found no evidence for their contribution to proliferative progenitor cells.

PAX7⁺ Cells Regenerate Muscle in Axolotl

Considering the lack of myofiber contribution to the axolotl limb regenerate, we searched for the source of cells for muscle regeneration. Previously, labeling of limb myofibers plus satellite cells via embryonic transplantation (green fluorescent protein labeled presomitic mesoderm transplant; GFP-PSM) resulted in robust contribution of GFP⁺ cells to the regenerated limb muscle (Kragl et al., 2009; Nacu et al., 2013). We confirmed here that the GFP⁺ nuclei were MEF2C⁺ (83% ± 2.7%) and PAX7⁺ (12% ± 2.3%) (n = 4, 277 ± 33 cells per section) (Figures 5A–5E). Since our above data indicated that myofibers make no contribution to the limb regenerate, this observation indicates that PAX7⁺ satellite cells are a major contributor to muscle regeneration in axolotl. To confirm the participation of PAX7⁺ cells in regeneration, we traced cells from the GFP-PSM labeled limbs (myofibers + satellite cells) into the blastema and found many GFP⁺ cells in the blastema (Figures 5F–5H, n = 5). Out of a total of 834 GFP⁺ blastema cells, 809 expressed PAX7 protein. This is in contrast to the labeling of Cherry⁺ myofibers alone (from the

LB-transplants) that gave no colocalization of muscle-derived Cherry⁺ signal with PAX7⁺ cells in the blastema (Figures S7D–S7F). These results indicate that PAX7⁺ cells are quantitatively the major contributors to muscle regeneration in the axolotl.

To further assess the proliferating status of the PSM-derived GFP⁺ cells in the blastema, we injected EdU in pulses prior to blastema collection, resulting in significant incorporation of the nucleotide analog in the blastema (Figure 5I). We corroborated colocalization of the nucleotide analog EdU with GFP in different areas of the blastema (Figures 5J and 5K). Furthermore, we immunostained for PCNA and found abundant GFP⁺ cells expressing this proliferation marker (Figure 5L). Taken together our data indicate that PAX7⁺ satellite cells from the mature limb produce proliferative, PAX7⁺ muscle progenitors of the limb blastema.

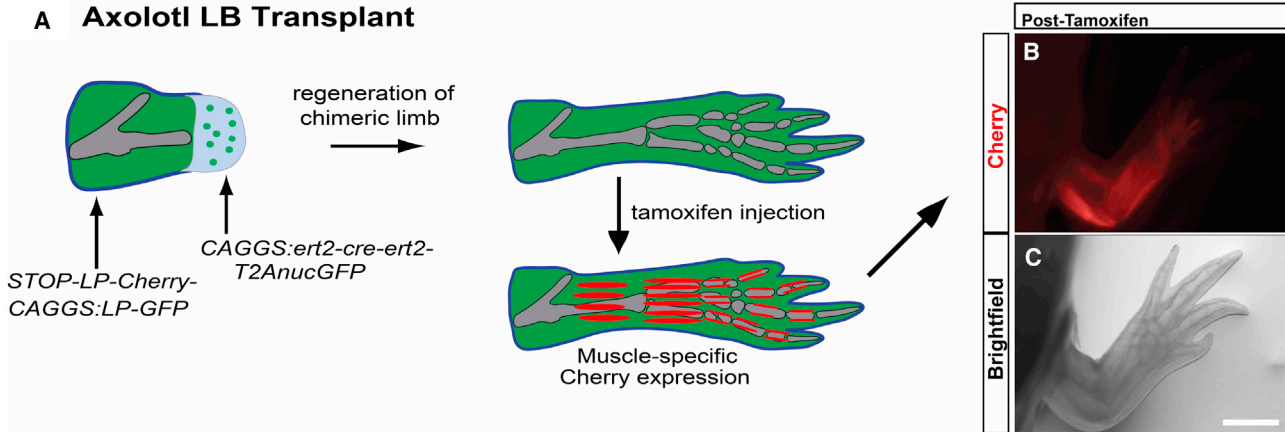
In the axolotl, proliferating PAX7⁺ cells are found abundantly and broadly distributed in the midbud limb blastema, consistent with their role as the muscle progenitors for limb regeneration (Figures 6G and 6H). In contrast, by midbud blastema stages the adult and larval newt limb blastema was devoid of PAX7⁺ cells (Figures 6A–6F), although PAX7⁺ cells had been described in the very early stages of newt limb regeneration (Morrison et al., 2006), probably representing satellite cells activated by muscle injury. We further compared the molecular profile of axolotl versus newt cells by examining myogenic determinants in isolated YFP⁺ and GFP⁺ cells from the newt and axolotl blastemas, respectively, by RT-PCR. These experiments confirmed that *Pax7* was not expressed in YFP⁺ cells arising from dedifferentiation in the newt blastema while *Pax7* was expressed in GFP⁺ cells isolated from satellite-cell-derived axolotl limb blastema cells (Figure 6I). Interestingly, cells from both axolotl and newt blastemas expressed *Myf5* but not two other myogenic determinants, *Myogenin* and *Mrf4* (Figure 6I). These results highlight fundamental differences in the cellular composition of the axolotl and newt limb blastema.

To address whether the difference between the two species reflects the special neotenic character of the axolotl, we forcibly metamorphosed axolotls and then analyzed limb muscle regeneration (Figure 7). Postmetamorphic axolotls were electroporated to specifically label limb myofibers as described for Figure 1 and Figure 3. We examined cross-sections of electroporated mature limbs and confirmed that only myofiber nuclei were expressing YFP. When we examined regenerated limbs for contribution of labeled muscle to the regenerate, we only observed YFP⁺ cells proximally to the amputation plane (n = 3, 190 nuclei) (Figures 7A–7C). To confirm this result, we metamorphosed animals that had been LB transplanted and tamoxifen-injected as described in Figure 4 (Figure 7D). Upon amputation, the

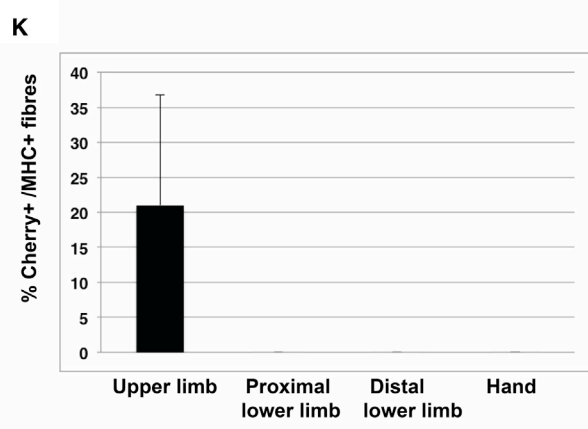
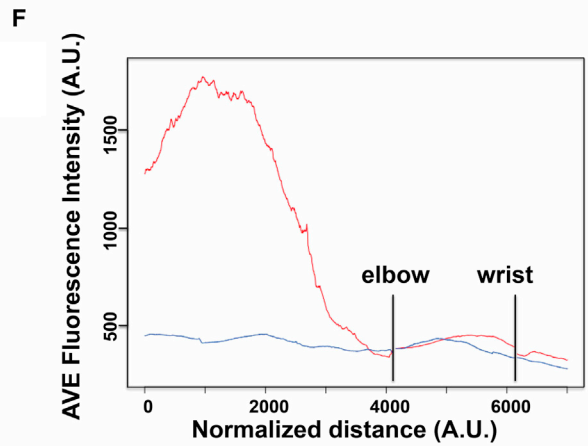
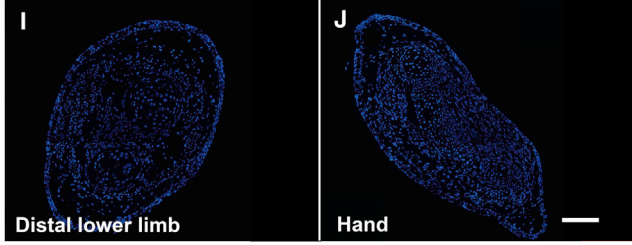
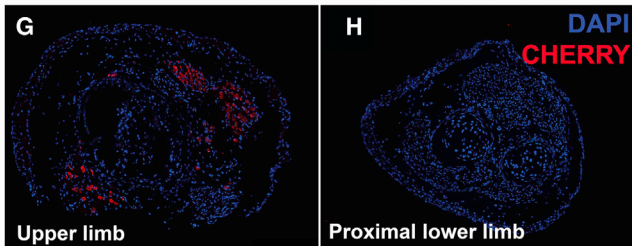
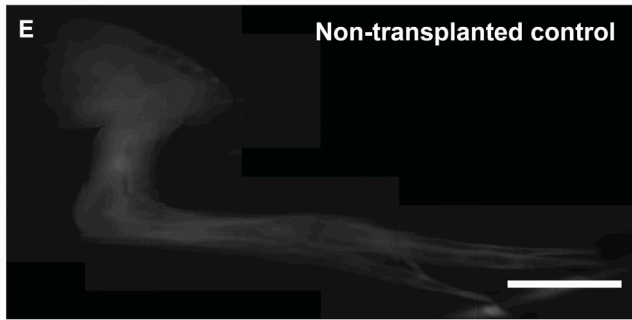
Figure 3. Larval Axolotls Show No Contribution of YFP⁺ Muscle Cells to New Muscle during Limb Regeneration

(A) Schematic outline of the experimental paradigms.
 (B–D) Colocalization of YFP⁺ nuclear signal (green) with MEF2C (white) by immunofluorescence detection. All nuclei (732 out of 732) counted were MEF2C⁺ (n = 6 limbs). Arrows indicate YFP⁺MEF2C⁺ double-positive cells.
 (E) 3D rendering of upper limb region electroporated with the abovementioned expression plasmids and immunostained for MHC (red). YFP⁺ nuclei closely associate with the MHC⁺ myofibers.
 (F) Upper arm muscle was labeled via coelectroporation of *MCK:cre*, *CAGGS:loxpCHERRY-STOPlloxp-H2BYFP*, and *CMV:Top2-transposase* expression plasmids. Whole-mount YFP fluorescence image of regenerated limb at 33 days is shown, showing nuclear expression in the upper limb but no visible YFP⁺ nuclei in the lower arm and hand. White line indicates amputation plane.
 (G) Number of YFP⁺ nuclei in upper limb, lower limb, and hand in 90-day regenerates counted after sectioning of limbs.
 Scale bars, (B)–(D): 50 μm; (E): 100 μm; (F): 2 mm.

A Axolotl LB Transplant



Regenerated Limb



(legend on next page)

regenerated limb showed no muscle labeled in lower limb or hand (Figure 7E, $n = 4$). Longitudinal sections of the limb regenerate confirmed the lack of Cherry⁺ myofibers in the lower limb or hand muscle (Figures 7F–7H).

DISCUSSION

Our fate mapping experiments showed an unexpected difference in the occurrence of myofiber dedifferentiation during limb regeneration in two salamander species. In the newt, labeled myofibers generated PAX7⁻, proliferative cells in the blastema that contributed exclusively to regenerated myofibers. Indeed, the newt limb blastema is essentially devoid of PAX7⁺ cells except for proximal regions at very early stages after amputation. In axolotl, labeled myofibers gave rise neither to proliferative cells in the blastema nor to regenerated myofibers at later stages. In contrast, our muscle grafting data indicate that axolotl limb muscle regeneration occurs by the recruitment of abundant PAX7⁺ cells from the mature tissue into the blastema, where they proliferate. The vast majority of myogenic blastema cells express PAX7 and are derived from PAX7⁺ satellite cells.

We have performed parallel electroporation experiments in the two species and obtained clearly different contributions of myonuclei to the regenerating limb. The lack of myofiber contribution in axolotl was confirmed using germline transgenically integrated cassettes where the efficiency of muscle labeling was at least as high as in the newt experiments: 9% of MHC⁺ myofiber nuclei expressed the labeling cassette in the axolotl experiments, compared to 5% in the newt. Another consideration was the life cycle of the animals. The axolotl is a neotenic animal in which larval features such as the gills are retained throughout life, and a question was whether the axolotl tracing results reflected a larval mode of regeneration. However, no contribution of labeled myofibers to the regenerate was observed in the postmetamorphic axolotl. Complementarily, no PAX7⁺ cells were found in the larval newt midbud blastema, revealing concrete molecular differences in the composition of the limb blastema between the two species.

In newt, myofiber-derived cells contributed to regenerated muscle and we so far found no evidence of contribution to

cartilage, consistent with our RT-PCR data showing that dedifferentiated YFP⁺ cells in the newt blastema express *Myf5* mRNA. Previous experiments tracking clonally cultured newt satellite cell progeny after limb implantation described contribution to cartilage in addition to skeletal muscle (Morrison et al., 2010). On the other hand, tracking of endogenous muscle and satellite cells in the axolotl showed no contribution to cartilage. We currently do not know whether newt satellite cells truly have a unique, broad potential to form cartilage, or whether experimental circumstances due to the culturing and implantation of the newt satellite cells could have influenced their properties. In vivo tracing studies specifically targeting endogenous satellite cells would clarify this issue. At present it is technically not possible in the newt because we were unable to transfect/label endogenous satellite cells in the newt limb. Similarly, in the future, it would be important to exclusively lineage trace satellite cells in axolotls to confirm their role in muscle regeneration, and to characterize the active transcriptional programs in these cells.

Newts and axolotls were separated from each other approximately 100 million years ago (Steinfartz et al., 2007). Although the ability of adult limb regeneration is a unique feature of salamanders among tetrapods (Simon and Tanaka, 2013), our observations suggest that microevolutionary selection pressures have led to divergent implementation of muscle dedifferentiation in these two species. It is important to note that adult newts can regenerate the lens of the eye by dedifferentiation of the pigmented epithelial cells of the iris (Grogg et al., 2005). Unlike newts, axolotls are able to regenerate the lens only during an early developmental time window of 2 weeks starting at the limb bud stage (Suetsugu-Maki et al., 2012).

The capacity to regenerate complex body parts is limited among vertebrates but not exclusive to salamanders: zebrafish can regrow amputated fins and larval frogs regenerate their limbs and tails. Cell tracking experiments in these animals showed varying manifestation of cellular dedifferentiation. New muscle arises from satellite cells and not from preexisting myofibers during tail regeneration in tadpoles (Gargioli and Slack, 2004; Rodrigues et al., 2012). In contrast, fin regeneration involves dedifferentiation of osteoblasts and heart regeneration involves

Figure 4. Tracing Using Germline Transgenic *loxP* Reporter Axolotls Yields No Evidence for Limb Myofibers Contributing to the Regenerated Limb

(A) *Cre-loxP*-based genetic labeling of axolotl limb muscle via blastema transplantation (Axolotl LB Transplant): schematic of experimental procedure. A 6-day or 10-day blastema from a *CAGGS:ert2-cre-ert2-T2A-nucGFP* transgenic animal was grafted onto the upper arm stump of a *CAGGS:loxP-GFP-STOP-loxP-Cherry* animal and allowed to regenerate (or vice versa). After at least 3 weeks of regeneration, animals were injected with tamoxifen. Since myofibers form from the fusion of myoblasts, they are the only chimeric cell type where the ERT2-CRE-ERT2 protein and the *loxP* reporter were found in the same cell and therefore expressed Cherry protein. All the remaining mononucleate cells (e.g., satellite cells) have either one or the other genotype and do not convert to Cherry expression upon tamoxifen administration.

(B and C) Fluorescence and brightfield image of a limb after tamoxifen injection. Cherry fluorescence is visible in upper and lower limb myofibers.

(D) LB transplant after regeneration showing no muscle contribution to the regenerate. White line denotes the amputation plane.

(E) Contralateral nontransplanted control limb to that shown in (D).

(F) Cherry fluorescence intensity graphs along the proximal-to-distal limb axis for samples shown in (D) and (E). Red line depicts the limb in (D) while blue line represents fluorescence intensity of the limb in (E). Pixel intensity across the width of the limb was averaged at every proximo-distal position to yield a single line intensity graph along the proximo-distal axis.

(G–J) Cross-sections from regenerated limb showing the distribution of Cherry⁺ muscle at (G) the upper arm proximal to amputation plane, (H) the proximal lower arm, (I) the distal lower arm, and (J) the hand. No Cherry⁺ cells were found at the lower arm and hand level, indicating that myofibers do not contribute to de novo myogenesis during axolotl limb regeneration.

(K) Fraction of Cherry⁺ myofibers (as visualized by anti-MHC immunofluorescence staining) in upper arm, proximal lower arm, distal lower arm, and hand. Data are presented as mean \pm SEM ($n = 3$).

Scale bars, (B) and (C): 1 mm; (D) and (E): 2 mm, (G–J): 200 μ m. See also Figures S4, S5, S6, and S7.

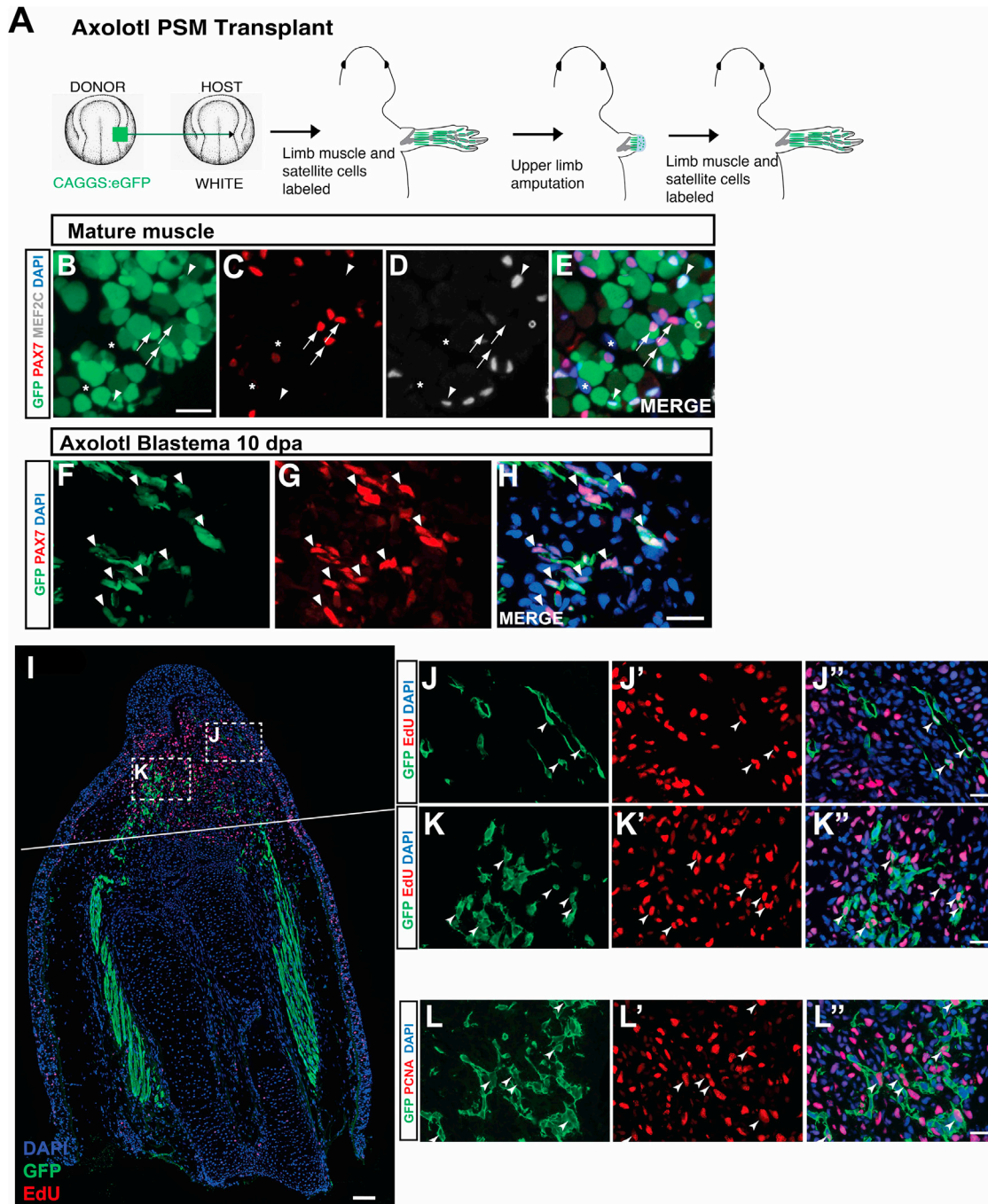


Figure 5. Tracing Using Presomitic Mesoderm Transplants in Axolotls Shows that PAX7⁺ Cells Contribute to the Limb Blastema

(A) Labeling and tracking of PAX7⁺ cells during limb regeneration. To label limb myofibers plus satellite cells, presomitic mesoderm (PSM) was transplanted from a GFP transgenic embryo to a white (nontransgenic) host and allowed to develop limbs. Schematic image of a PSM transplanted animal is shown. After amputation through a labeled region, a limb with green muscle and satellite cells is regenerated.

(B–E) Cross-section of the mature limb from PSM-labeled animal immunostained for MEF2C, a transcription factor expressed in differentiated muscle cells, and PAX7, a transcription factor found in the muscle satellite cells. Arrows label PAX7⁺GFP⁺ cells while arrowheads label MEF2C⁺GFP⁺ cells. Asterisks show nuclei negative for any labeling.

(F–H) A 10-day upper arm blastema (longitudinal section) from a PSM-labeled animal. All GFP⁺ cells in the blastema are PAX7⁺ (arrowheads). GFP (F), PAX7 (G).

(I) Longitudinal section of a 10-day blastema from a PSM transplant immunostained for GFP and EdU. Solid line shows amputation plane.

(J–J'' and K–K'') High magnification of inserts in (I) showing colocalization of GFP⁺ cells with EdU (arrowheads).

(L–L'') Colocalization of GFP⁺ cells and PCNA in the 10-day blastema (arrowheads).

Scale bars: (B)–(H) and (J)–(L): 50 μm; (I): 100 μm.

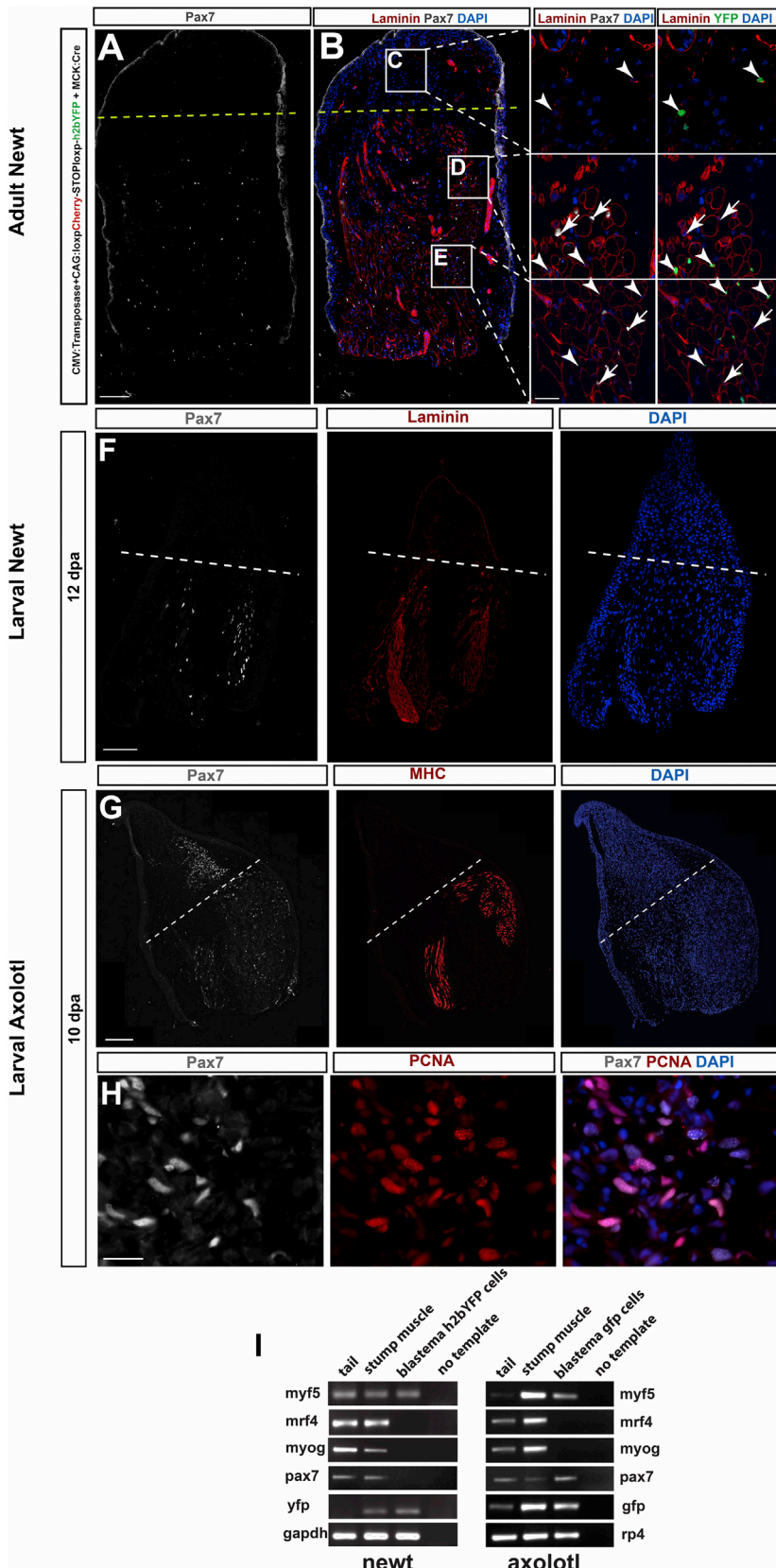


Figure 6. Abundance versus Lack of PAX7⁺ Cells in Axolotl and Newt Blastemas, Respectively

(A–E) Distribution of PAX7⁺ cells in the adult newt limb mesenchyme 14 days after amputation shows lack of PAX7 expression in the blastema. Note the background staining in the skin. (B–E) Distribution of PAX7⁺ cells in relation to myofibers (indicated by laminin staining) and to YFP⁺ cells deriving from muscle (C, blastema, D and E, limb stump). Arrows point to PAX7⁺ nuclei and arrowheads point to YFP⁺/PAX7[−] nuclei. Dashed lines indicate the amputation plane. (F) Absence of PAX7⁺ cells in the premetamorphic, larval newt limb blastema. Images show the distribution of PAX7⁺ cells in a 12-day-old blastema. Dashed lines indicate the amputation plane. (G) Abundance of PAX7⁺ cells in the premetamorphic, larval axolotl limb blastema. Images show the distribution of PAX7⁺ cells in a 10-day-old blastema. Dashed line indicates the amputation plane. (H) PCNA-expressing PAX7⁺ in the axolotl limb blastema. (I) Difference in molecular profile of myofiber-derived blastema cells from newt with PSM-derived blastema cells from axolotl. PCR was performed with cDNA from the tail, stump muscle, and blastema YFP⁺ or GFP⁺ cells from newt and axolotl, respectively. *Pax7* is not expressed in myofiber-derived cells in the newt blastema, whereas it is expressed in axolotl muscle-derived blastema cells. Other myogenic factors show similar regulation in newt and axolotl. Scale bars: (A), (F), and (G): 200 μm; (C)–(E) and (H): 20 μm.

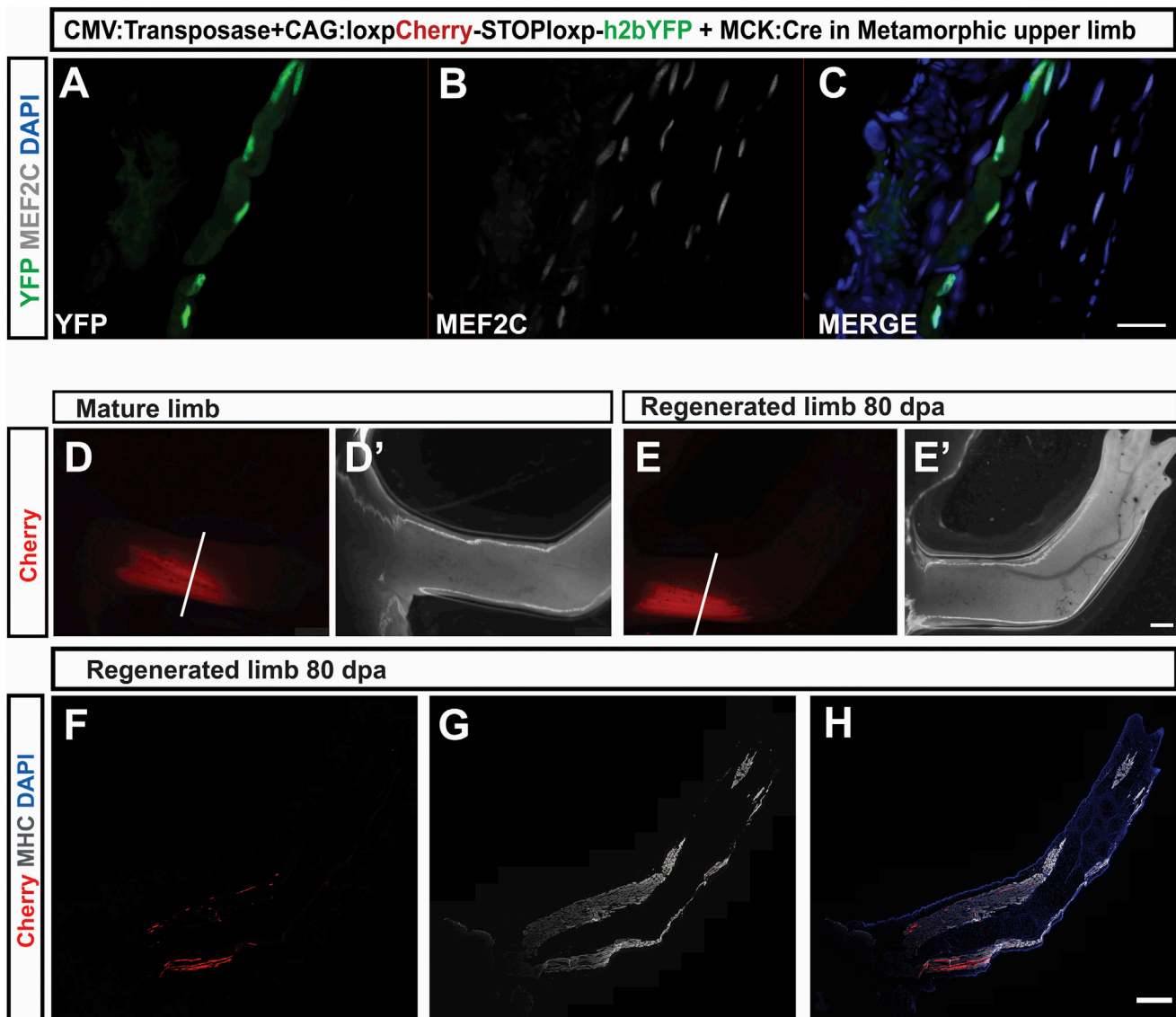


Figure 7. No Contribution of Myofiber-Derived Cells to Regeneration in Postmetamorphic Axolotl

(A–C) Colocalization of YFP⁺ nuclear signal with MEF2C in the upper limb proximal to the amputation plane in regenerated limbs in postmetamorphic animals. (D–D') Animals with limbs labeled by LB transplants were injected with thyroxine to induce metamorphosis and amputated in the upper limb. Fluorescence and brightfield image of a limb from a metamorphic animal with myofibers labeled is shown. White line marks the amputation plane.

(E and E') Fluorescence and brightfield image of the regenerated limb.

(F–H) Longitudinal section of the metamorphic regenerated limb immunostained for MHC. Cherry⁺ myofibers are found only in the upper arm and not in the lower arm or hand.

Scale bars, (A)–(C): 50 μ m; (D)–(H): 1 mm.

proliferation of cardiomyocytes in zebrafish (Jopling et al., 2010; Kikuchi et al., 2010; Knopf et al., 2011; Singh et al., 2012; Sousa et al., 2011). These observations along with recent cell tracing work in other vertebrate and invertebrate model organisms underscore the existence of a variety of cellular processes for blastema formation during regeneration (Eisenhoffer et al., 2008; Wagner et al., 2011). Understanding the underlying mechanisms may have significant implications for regenerative medicine (Blau and Pomerantz, 2011).

Taken together, our results demonstrate the flexibility and diversity of cellular mechanisms, even among salamanders,

used to arrive at successful regeneration, implying that multiple strategies are feasible for inducing muscle and limb regeneration in adult tetrapods.

EXPERIMENTAL PROCEDURES

Animals and Procedures

Red-spotted newts, *Notophthalmus viridescens*, were supplied by Charles D. Sullivan Co. (Nashville, TN, USA). Axolotls, *Ambystoma mexicanum*, were bred in our CRTD facility. Animals were anesthetized by being placed in an aqueous solution of ethyl 3-aminobenzoate methanesulfonate (Sigma). The CAGGS:loxpGFP-STOPlloxpCherry and CAGGS:ert2-cre-ert2-T2A-nucGFP

transgenic axolotls were generated via Scel meganuclease assisted plasmid injection, as described in [Khattak et al. \(2009\)](#), [Sobkow et al. \(2006\)](#), and the [Supplemental Experimental Procedures](#). All surgical procedures were performed according to the European Community and local ethics committee guidelines.

Injections and Electroporations

Plasmid preparation and injection procedures are provided in the [Supplemental Experimental Procedures](#).

Blastema Transplants

Donor Blastema Formation

The left or right forelimb of each animal was cut in the midupper arm and bone was trimmed to allow wound epidermis to form properly and to allow blastema to form.

Blastema Transplantation

The donor blastema was sliced off at day 6 and transplanted to an ipsilateral amputated upper limb. The transplanted blastema naturally adhered to the host due to the presence of clotted blood at the transplantation site. Limbs were allowed to fully regenerate. Different combinations of transplants were performed to validate our method. Donor Inducible Cre, Host *loxP* Cherry, $n = 20$; Donor *loxP* Cherry, Host Inducible Cre, $n = 13$. As controls, Donor Inducible Cre, Host White sibling of *loxP* Cherry, $n = 3$; Donor *loxP* Cherry, Host white sibling of Inducible Cre $n = 6$. The rationale behind this protocol is to have a combination of cells bearing the two different genes in the blastema formation. These two sets of cells would fuse during myogenesis, giving rise to myofibers containing both sets of genes that would only recombine after addition of tamoxifen ([Figure S4A](#)). In all cases, one limb of the animal was used for transplantation and the contralateral limb was left as a control.

Tamoxifen Injection

To induce Cre recombination, tamoxifen was injected i.p. at a concentration of 5 μg per 100 mg of body weight. Red fibers could be observed after 3 days of injection.

Limbs with visible red myofibers were amputated in the mid-upper arm 10 to 14 days after tamoxifen injection. The amputated limb (first regenerate) was fixed and processed for validation of the method. The right limb was also amputated and used as a control. Ten days after amputation, some of the blastemas were dissected out and fixed for analysis ($n = 12$). The remaining animals were left intact to allow the full limb to regenerate (second regenerate).

Embryonic Transplants

Embryonic transplants were carried as described previously in [Kragl et al. \(2009\)](#), [Nacu et al. \(2009\)](#), and the [Supplemental Experimental Procedures](#).

Metamorphosis of Axolotls

Animals of 10 cm were injected under the skin of the upper thoracic cavity with L-Thyroxine (Sigma T2376) at a concentration of 1.5 μg per gram of body weight. The first visible signs of gill regression were observed at 7 to 10 days postinjection. Metamorphosed animals were then kept in low water and fed fish pellets.

Immunohistochemistry, Whole-Mount Immunostaining, and Image Processing

Tissue processing, immunostaining, and microscopy procedures are provided in the [Supplemental Experimental Procedures](#).

Tissue Dissociation and RT-PCR

Newt limbs were dissociated according to ([Morrison et al., 2006](#)). Newt and axolotl blastemas were dissociated into single cells ([Kragl et al., 2009](#)), and YFP⁺ and GFP⁺ cells were picked up for further RT-PCR analysis. The tissue dissociation and RT-PCR procedures are provided in the [Supplemental Experimental Procedures](#).

SUPPLEMENTAL INFORMATION

Supplemental Information for this article includes Supplemental Experimental Procedures and seven figures and can be found with this article online at <http://dx.doi.org/10.1016/j.stem.2013.11.007>.

ACKNOWLEDGMENTS

We are grateful to Heino Andreas, Jitka Michling, Christel Junghans, Sabine Moegel, and Beate Gruhl for dedicated animal care. We thank Dunja Knapp and Serghei Novojilev for advice. Thanks to Joshua Currie for advice and for creating the graphical abstract. Thanks to Christopher Antos, and Ezio Bonifacio, Jeremy Brockes, and Peter Currie for comments on the manuscript. The work from E.M.T.'s lab was supported by grants from the Volkswagen Foundation, DFG (TA 274/2-2, TA 274/3-1, TA 274/3-2, TA 274/5-1), an ERC Advanced Investigator Award, central funds from the MPI-CBG, and CRTD. The work from the Simon lab was supported by grants from Cancerfonden, the Swedish Research Council, ERC, and the Wenner-Gren Foundation.

Received: May 1, 2013

Revised: September 12, 2013

Accepted: November 5, 2013

Published: November 21, 2013

REFERENCES

- Blau, H.M., and Pomerantz, J.H. (2011). Re"evolutionary" regenerative medicine. *JAMA* 305, 87–88.
- Calve, S., and Simon, H.G. (2011). High resolution three-dimensional imaging: Evidence for cell cycle reentry in regenerating skeletal muscle. *Dev. Dyn.* 240, 1233–1239.
- Calve, S., Odelberg, S.J., and Simon, H.G. (2010). A transitional extracellular matrix instructs cell behavior during muscle regeneration. *Dev. Biol.* 344, 259–271.
- Duckmanton, A., Kumar, A., Chang, Y.T., and Brockes, J.P. (2005). A single-cell analysis of myogenic dedifferentiation induced by small molecules. *Chem. Biol.* 12, 1117–1126.
- Echeverri, K., Clarke, J.D., and Tanaka, E.M. (2001). In vivo imaging indicates muscle fiber dedifferentiation is a major contributor to the regenerating tail blastema. *Dev. Biol.* 236, 151–164.
- Eisenhoffer, G.T., Kang, H., and Sánchez Alvarado, A. (2008). Molecular analysis of stem cells and their descendants during cell turnover and regeneration in the planarian *Schmidtea mediterranea*. *Cell Stem Cell* 3, 327–339.
- Gargioli, C., and Slack, J.M. (2004). Cell lineage tracing during *Xenopus* tail regeneration. *Development* 131, 2669–2679.
- Grogg, M.W., Call, M.K., Okamoto, M., Vergara, M.N., Del Rio-Tsonis, K., and Tsonis, P.A. (2005). BMP inhibition-driven regulation of six-3 underlies induction of newt lens regeneration. *Nature* 438, 858–862.
- Hay, E.D. (1959). Electron microscopic observations of muscle dedifferentiation in regenerating *Amblystoma* limbs. *Dev. Biol.* 1, 555–585.
- Iten, L.E., and Bryant, S.V. (1973). Forelimb regeneration from different levels of amputation in the newt, *Notophthalmus viridescens*: length, rate and stages. *Roux' Arch. Entwicklunsgmech. Org.* 173, 263–282.
- Jaynes, J.B., Johnson, J.E., Buskin, J.N., Gartside, C.L., and Hauschka, S.D. (1988). The muscle creatine kinase gene is regulated by multiple upstream elements, including a muscle-specific enhancer. *Mol. Cell. Biol.* 8, 62–70.
- Jopling, C., Sleep, E., Raya, M., Martí, M., Raya, A., and Izpisua Belmonte, J.C. (2010). Zebrafish heart regeneration occurs by cardiomyocyte dedifferentiation and proliferation. *Nature* 464, 606–609.
- Kawakami, K. (2007). Tol2: a versatile gene transfer vector in vertebrates. *Genome Biol.* 8 (Suppl 1), S7.
- Khattak, S., Richter, T., and Tanaka, E.M. (2009). Generation of transgenic axolotls (*Ambystoma mexicanum*). *Cold Spring Harb Protoc* 2009, pdb prot5264.

- Khattak, S., Schuez, M., Richter, T., Knapp, D., Haigo, S.L., Sandoval-Guzmán, T., Hradlikova, K., Duemmler, A., Kerney, R., and Tanaka, E.M. (2013). Germline transgenic methods for tracking cells and testing gene function during regeneration in the axolotl. *Stem Cell Reports* 1, 90–103.
- Kikuchi, K., Holdway, J.E., Werdich, A.A., Anderson, R.M., Fang, Y., Egnaczyk, G.F., Evans, T., Macrae, C.A., Stainier, D.Y., and Poss, K.D. (2010). Primary contribution to zebrafish heart regeneration by *gata4*(+) cardiomyocytes. *Nature* 464, 601–605.
- Knopf, F., Hammond, C., Chekuru, A., Kurth, T., Hans, S., Weber, C.W., Mahatma, G., Fisher, S., Brand, M., Schulte-Merker, S., and Weidinger, G. (2011). Bone regenerates via dedifferentiation of osteoblasts in the zebrafish fin. *Dev. Cell* 20, 713–724.
- Kragl, M., Knapp, D., Nacu, E., Khattak, S., Maden, M., Epperlein, H.H., and Tanaka, E.M. (2009). Cells keep a memory of their tissue origin during axolotl limb regeneration. *Nature* 460, 60–65.
- Kumar, A., Velloso, C.P., Imokawa, Y., and Brockes, J.P. (2000). Plasticity of retrovirus-labelled myotubes in the newt limb regeneration blastema. *Dev. Biol.* 218, 125–136.
- Kumar, A., Velloso, C.P., Imokawa, Y., and Brockes, J.P. (2004). The regenerative plasticity of isolated urodele myofibers and its dependence on *MSX1*. *PLoS Biol.* 2, E218.
- Lo, D.C., Allen, F., and Brockes, J.P. (1993). Reversal of muscle differentiation during urodele limb regeneration. *Proc. Natl. Acad. Sci. USA* 90, 7230–7234.
- Morrison, J.I., Löff, S., He, P., and Simon, A. (2006). Salamander limb regeneration involves the activation of a multipotent skeletal muscle satellite cell population. *J. Cell Biol.* 172, 433–440.
- Morrison, J.I., Borg, P., and Simon, A. (2010). Plasticity and recovery of skeletal muscle satellite cells during limb regeneration. *FASEB J.* 24, 750–756.
- Nacu, E., Knapp, D., Tanaka, E.M., and Epperlein, H.H. (2009). Axolotl (*Ambystoma mexicanum*) embryonic transplantation methods. *Cold Spring Harb Protoc* 2009, pdb prot5265.
- Nacu, E., Glausch, M., Le, H.Q., Damanik, F.F., Schuez, M., Knapp, D., Khattak, S., Richter, T., and Tanaka, E.M. (2013). Connective tissue cells, but not muscle cells, are involved in establishing the proximo-distal outcome of limb regeneration in the axolotl. *Development* 140, 513–518.
- Odelberg, S.J., Kollhoff, A., and Keating, M.T. (2000). Dedifferentiation of mammalian myotubes induced by *msx1*. *Cell* 103, 1099–1109.
- Rodrigues, A.M., Christen, B., Martí, M., and Izpisua Belmonte, J.C. (2012). Skeletal muscle regeneration in *Xenopus* tadpoles and zebrafish larvae. *BMC Dev. Biol.* 12, 9.
- Rossi, S.G., Vazquez, A.E., and Rotundo, R.L. (2000). Local control of acetylcholinesterase gene expression in multinucleated skeletal muscle fibers: individual nuclei respond to signals from the overlying plasma membrane. *J. Neurosci.* 20, 919–928.
- Simon, A., and Tanaka, E.M. (2013). Limb regeneration. *Wiley Interdiscip Rev Dev Biol* 2, 291–300.
- Singh, S.P., Holdway, J.E., and Poss, K.D. (2012). Regeneration of amputated zebrafish fin rays from de novo osteoblasts. *Dev. Cell* 22, 879–886.
- Slack, J.M. (2006). Amphibian muscle regeneration—dedifferentiation or satellite cells? *Trends Cell Biol.* 16, 273–275.
- Sobkow, L., Epperlein, H.H., Herklotz, S., Straube, W.L., and Tanaka, E.M. (2006). A germline GFP transgenic axolotl and its use to track cell fate: dual origin of the fin mesenchyme during development and the fate of blood cells during regeneration. *Dev. Biol.* 290, 386–397.
- Sousa, S., Afonso, N., Bensimon-Brito, A., Fonseca, M., Simões, M., Leon, J., Roehl, H., Cancela, M.L., and Jacinto, A. (2011). Differentiated skeletal cells contribute to blastema formation during zebrafish fin regeneration. *Development* 138, 3897–3905.
- Steinfartz, S., Vicario, S., Arntzen, J.W., and Caccone, A. (2007). A Bayesian approach on molecules and behavior: reconsidering phylogenetic and evolutionary patterns of the Salamandridae with emphasis on *Triturus* newts. *J. Exp. Zool. B Mol. Dev. Evol.* 308, 139–162.
- Stocum, D.L., and Cameron, J.A. (2011). Looking proximally and distally: 100 years of limb regeneration and beyond. *Dev. Dyn.* 240, 943–968.
- Suetsugu-Maki, R., Maki, N., Nakamura, K., Sumanas, S., Zhu, J., Del Rio-Tsonis, K., and Tsonis, P.A. (2012). Lens regeneration in axolotl: new evidence of developmental plasticity. *BMC Biol.* 10, 103.
- Tanaka, E.M., Gann, A.A., Gates, P.B., and Brockes, J.P. (1997). Newt myotubes reenter the cell cycle by phosphorylation of the retinoblastoma protein. *J. Cell Biol.* 136, 155–165.
- Wagner, D.E., Wang, I.E., and Reddien, P.W. (2011). Clonogenic neoblasts are pluripotent adult stem cells that underlie planarian regeneration. *Science* 332, 811–816.